Journal of Physics:
Conference Series

PAPER • **OPEN ACCESS**

Flexible hot-film sensors for underwater wall shear stress measurement

To cite this article: Ziqiang Xiang *et al* 2026 *J. Phys.: Conf. Ser.* **3256** 012069

Flexible hot-film sensors for underwater wall shear stress measurement

Ziqiang Xiang[1,2], Qingshan Wu[1,2], Guanjun Liu[1,2,*]

[1] College of Intelligence Science and Technology, National University of Defense Technology, Changsha, Hunan 410073, P. R. China
[2] National Key Laboratory of Equipment State Sensing and Smart Support, National University of Defense Technology, Changsha, Hunan 410073, P. R. China.

[*]Corresponding author's e-mail: gjliu342@nudt.edu.cn

Abstract. Wall shear stress (WSS) measurement is essential for fluid dynamics research and the hydrodynamic optimization of Autonomous Underwater Vehicles (AUVs). However, conventional measurement techniques suffer from drawbacks such as intrusiveness, low spatial resolution, poor adaptability to curved surfaces, or high fabrication costs. To address these issues, this study develops a flexible hot-film sensor for underwater WSS measurement, fabricated via a low-cost screen-printing process using conductive carbon paste as the sensing element on a polyimide (PI) substrate, with a reliable waterproof packaging scheme designed for underwater stability. The sensor was integrated into a Constant Temperature Anemometer (CTA) circuit, and systematic calibration was conducted in a fully developed turbulent channel flow using the pressure drop method as the rigorous WSS reference, with the Darcy-Weisbach equation applied to calculate the actual WSS from measured pressure drops at different flow velocities. Key characterizations of the carbon-based sensitive material and the sensor's performance were carried out: the carbon paste exhibited a stable positive Temperature Coefficient of Resistance (TCR) of 3347 ppm/°C; the calibration curve of the sensor was fitted as $U = \sqrt{38.9679 + 31.3633\tau^{1/3}}$ with a high determination coefficient $R^2 = 0.971$; the sensor achieved a minimum resolution of 0.05 Pa, a response time of less than 0.35 s, and excellent cyclic stability with an almost unchanged baseline and consistent output after three loading cycles between 0.1 Pa and 1.4 Pa. This screen-printed flexible hot-film sensor features low fabrication cost, good conformability to non-planar surfaces, high sensitivity, fast dynamic response, and stable underwater performance, providing a reliable and practical solution for underwater WSS measurement, and showing great application potential in hydrodynamic research and AUV drag reduction optimization.

1. Introduction

Wall shear stress (WSS) measurement is fundamental to fluid dynamics, as it is closely associated with skin-friction drag [1], flow separation [2], and turbulence transition.[3] For the hydrodynamic optimization of naval Autonomous Underwater Vehicles (AUVs), accurate WSS quantification is critical to validating drag reduction strategies.[4], [5] Currently, various techniques have been established to measure WSS. But these approaches suffer from inherent limitations that restrict their practical applicability in underwater WSS measurement. Direct methods, such as floating element balances, enable the provision of direct force measurements but are susceptible to pressure gradients and mechanical vibrations. [6] Indirect methods, including Preston tubes and Stanton gauges, infer WSS from the law of the wall, yet are intrusive and inevitably perturb the local flow field [7]. Optical techniques like Particle Image Velocimetry (PIV) offer non-intrusive solutions [8]. However, they typically suffer from low spatial resolution in the near-wall region and require complex, expensive optical setups.

Hot-film thermal shear stress sensors have emerged as a dominant technique for underwater wall shear stress (WSS) measurement, due to their high sensitivity, high-frequency response, and low intrusiveness. [9] Conventional hot-film sensors are mostly fabricated via Micro-Electro-Mechanical Systems (MEMS) technology on rigid silicon substrates, and such sensors exhibit high measurement precision and excellent operational performance [10]. However, these rigid-based sensors cannot achieve conformal attachment to curved surfaces commonly found in hydrodynamic underwater applications. Flexible electronics technology provides an effective solution to this mounting challenge [11], and flexible sensors fabricated by MEMS technology have become a current research focus with promising application performance. [12] MEMS technology has inherent shortcomings for fabricating flexible sensors, including cumbersome fabrication processes, reliance on large and precision cleanroom equipment, and potential environmental pollution caused by pollutants generated in certain preparation steps. As a flexible electronics fabrication process, screen printing has been widely applied to the development of various flexible sensors, due to its prominent advantages of low cost, simple operation, and feasible large-scale fabrication. [13], [14] Although considerable progress has been made in the research of screen-printed sensors, relevant studies on hot-film thermal shear stress sensors for underwater working conditions remain relatively insufficient. The systematic research of screen-printed sensors in underwater environments is still limited.

In this study, we present the fabrication and comprehensive characterization of a flexible hot-film sensor for underwater applications. The sensor is fabricated using a screen-printing process with conductive carbon paste as the sensing element on a flexible PI substrate. A low-cost fabrication process and a reliable waterproof packaging scheme were developed to ensure stability in water. The sensor was then integrated into a Constant Temperature Anemometer (CTA) circuit and rigorously calibrated in a fully developed turbulent channel flow. The pressure drop method was employed to provide an accurate WSS reference for establishing the calibration curve. Finally, the static and dynamic performances, including minimum resolution, response time, and repeatability under cyclic loading, were experimentally evaluated.

2. Flexible Hot-Film Sensors

2.1. Working principle

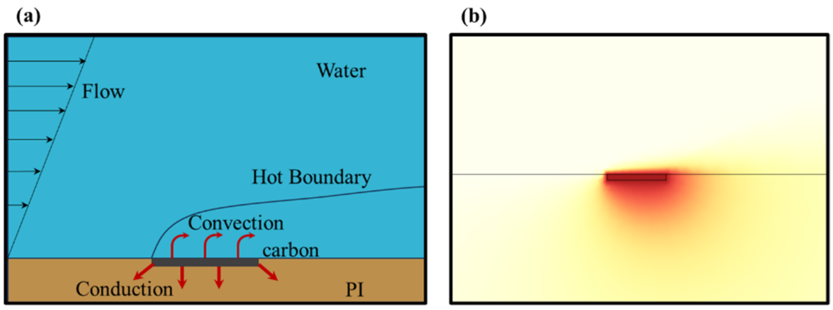

Figure 1. Working principle of the sensor: thermal distribution diagram. (a) Schematic diagram of underwater thermal film heat transfer. (b) Diagram of Underwater Heat Distribution Simulated by COMSOL.

The working principle of the sensor is illustrated in Figure 1(a). The sensor is based on the principle of convective heat transfer. When a voltage is applied to the sensitive resistor of the sensor, the sensitive material's temperature rises due to the Joule heating effect. At this point, the heat dissipation of the sensitive material is divided into three components: 1) convective heat transfer to the water flow; 2) heat conduction to the substrate (essentially constant); 3) radiative heat transfer (negligible). In order to better present the schematic diagram of the underwater thermal distribution, a COMSOL-based physical field simulation was carried out to investigate the heat dissipation mechanism of the underwater hot-film sensor (see Figure 1(b)). It can be observed that most of the heat is transferred to the substrate via thermal conduction and carried away by the water via thermal convection, while the heat removed by thermal radiation is negligible. When the sensor operates under the constant-temperature mode and the water temperature is fixed, the heat conducted to the substrate is nearly independent of the flow velocity. In contrast, the heat removed by thermal convection increases with the rise of flow velocity. Therefore, the voltage required to maintain the constant temperature increases with the increment of heat loss. Heat loss via convective heat transfer is primarily related to the flow velocity boundary layer. In general, under the constant temperature mode, the wall shear stress is related to the applied voltage as follows [15]:

$$U^2 = A \cdot \tau^{1/3} + B$$

wherein, A and B are the to-be-calibrated coefficients, τ represents the wall shear stress, and U is the voltage applied on the sensor. Specifically, A is related to the sensor structure, the Temperature Coefficient of Resistance (TCR) of the sensitive material, and other relevant factors, while B is associated with the preset conditions. The higher the TCR of the material, the better the sensor's resolution. To this end, the definition of TCR is presented as follows:

$$TCR = \frac{R_2 - R_1}{T_2 - T_1}$$

In the above equation, T_1 and T_2 denote temperatures, and R_1 and R_2 are the corresponding resistances of the sensitive material at temperatures T_1 and T_2, respectively.

2.2. Design and Fabrication

The hot-film sensor was fabricated through a screen-printing process. The fabrication consists of three key steps: fabrication of silver conductive circuits, printing of carbon-based sensitive layer, and PI film encapsulation, as illustrated in Figure 2.

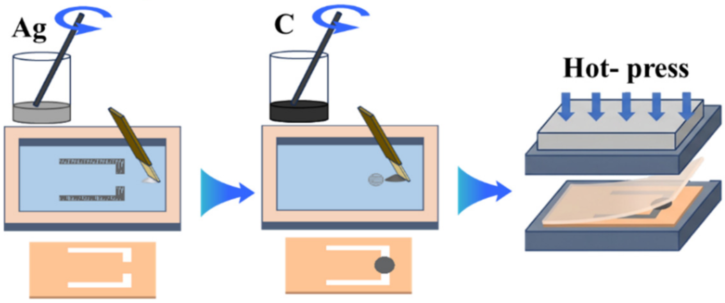

Figure 2. Preparation process of flexible hot film sensor.

Firstly, a clean and dry 25-um-thick PI substrate was selected as a temporary carrier. Place a 25 um PI film on a glass substrate to ensure the flatness and stability of each printed layer during the preparation process. Silver paste (the silver paste (LY508) was purchased from Shenzhen Yilai Technology Co., Ltd.) with high conductivity was screen-printed on the 25 um-thick PI substrate through a pre-designed stencil. The silver circuit served as the conductive wires and electrode circuits of the sensor. Then, the silver layer was sintered at 90 °C for 30 min to enhance its adhesion and conductivity. Subsequently, the carbon-based sensitive material (the carbon paste (CH50011F) was purchased from Shenzhen Selihui Co., Ltd. and was screen-printed on the designated area of the silver electrode, forming the core sensitive layer of the hot-film sensor. The carbon layer was then dried at 80 °C for 30 min to remove the solvent and ensure the structural integrity of the sensitive layer. Finally, a PI film was hot-pressed on the surface of the sensor to realize the encapsulation. The hot-pressing process was carried out at 150 °C with a pressure of 0.3 MPa for 20 min. The hot-pressing process achieved tight bonding between the PI film and the sensor surface while avoiding damage to the sensitive layer.

To evaluate the feasibility and reliability of the carbon-based material as the sensitive layer of the hot-film sensor, the measurement of the Temperature Coefficient of Resistance (TCR) of the carbon material was carried out. The TCR of the carbon-based sensitive material was measured using a high-precision resistance tester (Keithley 2400 Graphical Series Sourcemeter) combined with a temperature-controlled chamber. It can accurately control the ambient temperature and record the corresponding resistance change of the carbon layer. The test temperature range was set from 0 °C to 80 °C. The range of temperature covers the actual working temperature range of the sensor in underwater friction drag measurement. And the temperature was increased at a rate of 2 °C/min to ensure the stability of the resistance measurement. The test results show that the carbon-based sensitive material exhibits a stable positive TCR characteristic(~3347 ppm/°C, as shown in Figure 3).

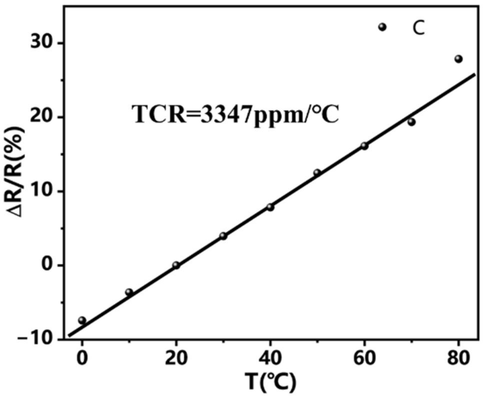

Figure 3. Diagram of the TCR of the carbon layer.

3. Wall shear stress measurement

3.1. Experiment setting

To achieve the measurement of wall shear stress, it is first necessary to apply predefined wall shear stress conditions. Therefore, the water tunnel setup, as shown in Figure 4, was adopted. A differential pressure gauge was mounted above the water tunnel, and the actual pressure drop across the wall can be derived from the readings of the differential pressure gauge.

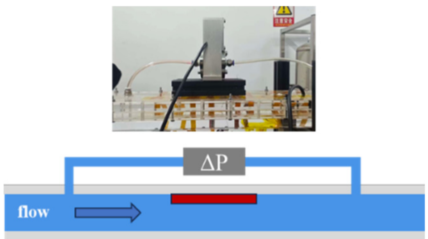

Figure 4. Schematic picture of measuring friction using the pressure drop method.

According to the Darcy-Weisbach equation [16], the relationship between the pressure drop inside the pipeline and the wall shear stress on the inner wall of the pipeline follows the following equation:

$$\tau = \frac{\Delta P \cdot b \cdot h}{2(b+h)L}$$

where b and h are the flow width and height of the rectangular pipe, respectively, and L is the axial distance between pressure tapings. For a square cross-section pipe (b=h). In the experimental conditions, the spacing L between the pressure taps connected to the differential pressure gauge is 400 mm, the width b of the flow channel is 60 mm, and the height h is 6 mm. Subsequently, the experimental conditions of the water tunnel were calibrated. After measurement, the pressure drops at every 0.1 m/s interval within the flow velocity range of 0–2.1 m/s was obtained, and the corresponding wall shear stress was calculated. Thus, the actual wall shear stress at different flow velocities has been obtained, as presented in Figure 5.

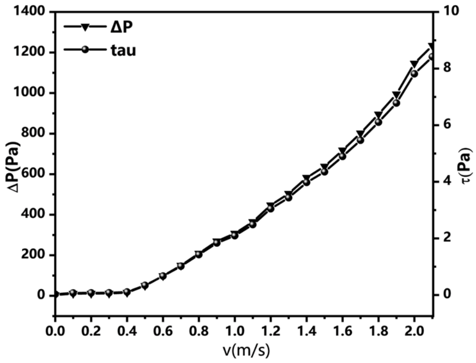

Figure 5. Curve graph of pressure drops and calculated wall friction stress at different flow rates.

3.2. Result

Subsequently, the sensor was mounted inside the water tunnel, and constant temperature measurement of the hot-film sensor was achieved via the constant temperature feedback circuit, as presented in Figure 6.

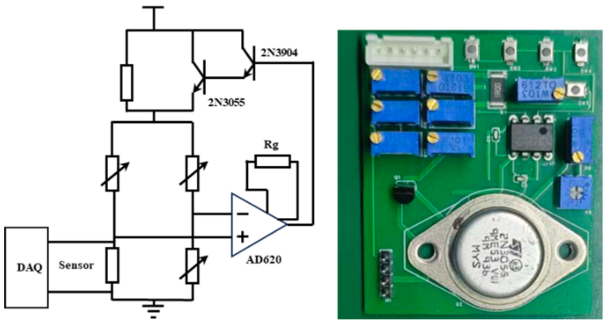

Figure 6. Schematic and physical diagram of a constant temperature circuit.

The AD620 instrumentation amplifier was adopted as the detection unit of the constant temperature bridge, since it features an extremely low offset voltage that can enhance the resolution under the conditions of low flow velocity and small signal differences. A feedback resistor of 10 Ω was selected for the AD620, yielding an amplification gain of 5000 times, which is sufficient to amplify the bridge output under the constant temperature difference condition. However, the AD620 has a relatively low load capacity; thus, the 2N3904 and 2N3905 transistors were configured to form a Darlington pair, which enables the achievement of a high load capacity even when the AD620 outputs a small current. Subsequently, the sensor was tested at different water flow velocities with a sampling time of 2 min, and the time-domain signal of the sensor was acquired. The time-domain sampling data for each segment were averaged to determine the sensor output. The abscissa represents the wall shear stress corresponding to each flow velocity, and the calibration curve of the sensor was thereby obtained (as shown in Figure 7).

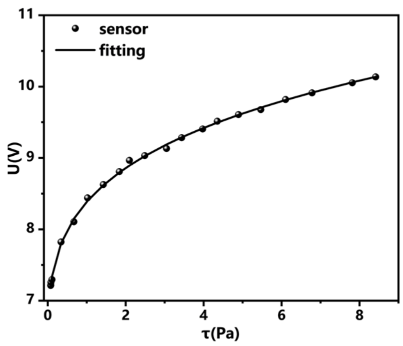

Figure 7. Diagram of the calibration of sensors.

The calibration curve was fitted, yielding $U = \sqrt{38.9679 + 31.3633\tau^{1/3}}$ with a determination coefficient $R^2 = 0.971$, which is generally consistent with the law expressed in Equation 1 above. In addition to calibrating the fabricated sensor, we characterized its fundamental performance (as shown in Figure 8). The first index is the minimum resolution of the sensor, which represents its ability to detect the minimum wall shear stress. According to our test results, at a flow velocity of 0.4 m/s (the minimum rotational speed of the water pump), the wall shear stress calculated from the differential pressure gauge increased from 0.10 Pa to 0.15 Pa, and the sensor exhibited a clearly distinguishable step response. Therefore, the minimum resolution is determined to be 0.05 Pa. Besides the minimum resolution, the response speed of the sensor is also an important characteristic, reflecting its sensitivity to rapid changes in wall shear stress. During our tests, the response time Δt of the sensor was measured to be 0.35 s. This value corresponds to the sensor detecting the variation in wall shear stress caused by the change in wall flow velocity. Considering that the adjustment of the pump rotational speed also requires a certain time, the actual response speed of the sensor is in fact faster than 0.35 s. Finally, the cycling performance of the sensor was evaluated. Maintaining a stable baseline without drift and a consistent response after several identical cycles is a crucial indicator of the sensor's stability. In this study, the sensor was subjected to three cycles between 0.1 Pa and 1.4 Pa. It was found that the baseline of the sensor remained nearly unchanged, and the sensor output was also highly consistent under the same wall shear stress conditions. These results demonstrate the good stability of the as-fabricated sensor.

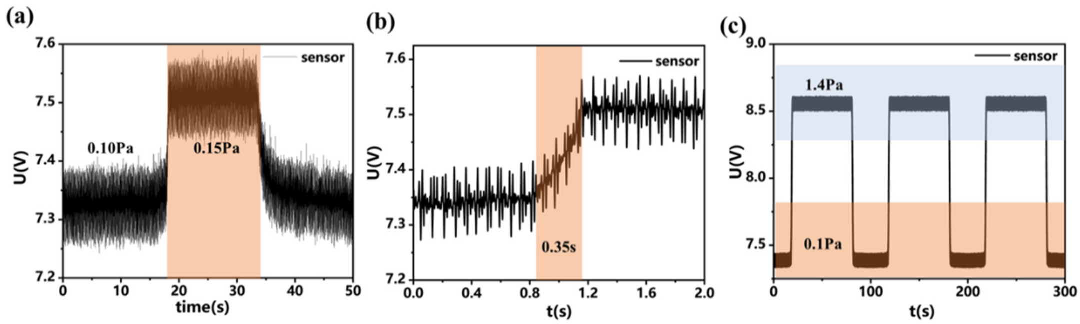

Figure 8. Basic performance characterization of sensors. (a) minimum resolution of sensors; (b) response time of sensors; (c) cyclic characteristics of sensors.

4. Conclusion

This paper presents an underwater wall shear stress hot-film sensor, which is fabricated on a flexible PI film via a low-cost screen-printing process combined with conductive carbon paste. The basic structure of the sensor is prepared by screen printing, and the temperature coefficient of resistance (TCR) of the carbon paste is measured to be 3347 ppm/°C. Subsequently, a water tunnel capable of providing reliable wall shear stress is established. The relationship between wall shear stress and pressure drop based on the pressure drop method is analyzed, and the sensor is calibrated in the water tunnel to obtain its calibration curve. Finally, the fundamental performance of the sensor is characterized. The sensor achieves a minimum resolution of 0.05 Pa and a response time of less than 0.35 s. After a period of cyclic operation, the sensor still maintains a stable output, demonstrating its excellent performance.

Acknowledgement

This work is supported by the State Key Laboratory Grant (6142003202401, WDZC20235250302) from the National Key Laboratory of Equipment State Sensing and Smart Support, the General Program of China Postdoctoral Science Foundation (2024M764286), the National Postdoctoral Researchers Support Program (Category C) (GZC20242270), and the National Natural Science Foundation of China (5227053453).

Journal of Physics: Conference Series **3256** (2026) 012069 doi:10.1088/1742-6596/3256/1/012069

References

[1] W. Li, Y. Fan, D. Modesti, and C. Cheng, "Decomposition of the mean skin-friction drag in compressible turbulent channel flows," J. Fluid Mech., vol. 875, pp. 101–123, Sep. 2019.
[2] Z. Bradshaw, "Remarks on the separation of Navier–Stokes flows," Nonlinearity, vol. 37, no. 9, p. 095023, Sep. 2024.
[3] O. Marxen and T. A. Zaki, "Turbulence in intermittent transitional boundary layers and in turbulence spots," J. Fluid Mech., vol. 860, pp. 350–383, Feb. 2019.
[4] J. Shi, H. Zhou, X. Feng, G. Tian, and Z. Lian, "Effect of the Biomimetic Spine-Covered Protrusions (BSCPs) Height and Arrangement on SUBOFF Bare Hull Model Drag," Arab. J. Sci. Eng., vol. 48, no. 3, pp. 2873–2888, Mar. 2023.
[5] Y. Gao, X. Li, J. Mei, D. Lu, and Y. Tang, "Hydrodynamic Numerical Analysis of AUV Underwater Docking with Conical Docking Bay," J. Mar. Sci. Eng., vol. 13, no. 9, p. 1645, Aug. 2025.
[6] Y. Liu et al., "A MEMS wall shear stress sensor with floating cover plate for aerospace flow monitoring in harsh environments," Microsyst. Nanoeng., vol. 11, no. 1, p. 183, Oct. 2025.
[7] N. Rajaratnam and D. Muralidhar, "Yaw Probe used as Preston Tube," Aeronaut. J., vol. 72, no. 696, pp. 1059–1060, Dec. 1968.
[8] J. Eppink and C. Yao, "Lensless particle image velocimetry," Exp. Fluids, vol. 65, no. 5, p. 73, May 2024.
[9] C. Ghouila-Houri et al., "High temperature gradient calorimetric wall shear stress micro-sensor for flow separation detection," Sens. Actuators Phys., vol. 266, pp. 232–241, Oct. 2017.
[10] S. O. Aleksic, N. S. Mitrovic, M. D. Lukovic, N. N. Obradovic, and M. D. Pavlovic, "Temperature Response, Time Delay, and Hysteresis Loop of Heat Loss Flowmeter Thermistors," IEEE Sens. J., vol. 25, no. 8, pp. 12695–12702, Apr. 2025.
[11] J. Guo et al., "Microfluidics for flexible electronics," Mater. Today, vol. 44, pp. 105–135, Apr. 2021.
[12] J. Zhang, X. Guan, X. Hu, M. Cai, and Y. Jiang, "A PDMS-Based Flexible Calorimetric Flow Sensor With Double-Bridge Technology," IEEE Sens. J., vol. 24, no. 22, pp. 36530–36538, Nov. 2024.
[13] C. Offenzeller, M. Knoll, B. Jakoby, and W. Hilber, "Screen Printed Thermal Flow Velocity Sensor for Microfluidic Devices Featuring Intrinsic Compensation of Spurious Heat Transfe," in 2019 20th International Conference on Solid-State Sensors, Actuators and Microsystems & Eurosensors XXXIII (TRANSDUCERS & EUROSENSORS XXXIII), Berlin, Germany: IEEE, Jun. 2019, pp. 2322–2325.
[14] C. Offenzeller, M. A. Hintermüller, M. Knoll, B. Jakoby, and W. Hilber, "Simultaneous Microfluidic Flow Velocity and Thermal Conductivity Measurement Utilizing Screen Printed Thermal Sensors," in 2019 IEEE SENSORS, Montreal, QC, Canada: IEEE, Oct. 2019, pp. 1–4.
[15] P. Pang et al., "Flexible Sensing Skin for Simultaneous Measurement of Wall Shear Stress, Flow Direction and Dynamic Pressure," in 2024 IEEE SENSORS, Kobe, Japan: IEEE, Oct. 2024, pp. 1–4.
[16] A. Abdulsamad and K. A. Abdulrazzaq, "Applying the WaterGEMS Software to Conduct a Comparison of the Darcy-Weisbach and Hazen-Williams Equations for Calculating the Frictional Head Loss in a Selected Pipe Network," J. Eng., vol. 29, no. 2, pp. 153–163, Feb. 2023.